Nonadiabatic effects in charge transfer in atom-surface scattering

Hongxiao Shao and Peter Nordlander
Department of Physics and Rice Quantum Institute, Rice University, Houston, Texas 77251-1892

David C. Langreth
Department of Physics and Astronomy, Rutgers University, Piscataway, New Jersey 08855-0849
(Received 1 February 1995; revised manuscript received 31 March 1995)

Using a recently developed many-body theory, we investigate the velocity dependence of charge transfer in atom-surface scattering. We show that under certain conditions, intra-atomic correlation effects can introduce nontrivial sources of nonadiabaticity. For situations where a sharp Kondo resonance is formed near the Fermi energy, the system can exhibit strong nonadiabatic effects even at low velocities. This nonadiabatic behavior is caused by the relatively long-time scale for the formation or survival of the Kondo peak.

I. INTRODUCTION

In recent years, there has been considerable theoretical and experimental interest in the charge-transfer processes that can occur when an atom or a molecule collides with a solid surface.[1–6] Charge-transfer processes are of crucial importance for the understanding of a number of important physical processes, such as sticking and desorption. From a theoretical point of view, the charge-transfer process represents an interesting physical problem in which nonadiabatic, nonequilibrium, and electron-correlation effects can be strong. The relative simplicity with which charge-transfer processes can be studied experimentally makes this field a very fertile area for the study of these effects.

Until recently, most of the theoretical investigations of charge-transfer reactions in atom-surface scattering have been based on the nondegenerate single-level Anderson model[7–9] where intra-atomic Coulomb interaction is neglected. For this model, the final population of the atomic states can be obtained in analytical form. Although theoretically appealing, this model is often too crude for the proper description of realistic systems. Even for the simplest systems, there will always be a degeneracy due to the spin of the electron. In typical situations, the intra-atomic Coulomb interaction would prevent more than one of the degenerate states from being occupied at the same time. In addition, intra-atomic interaction can introduce nontrivial many-body effects, such as the strongly correlated mixed valence or Kondo states in the system.

The multilevel or N-fold degenerate Anderson Hamiltonian is quite complex and an exact analytic solution is not possible even in equilibrium. Several approaches for the approximate solution of this time-dependent model with intra-atomic Coulomb interaction have been developed.[10–17] Recently the problem has attracted considerable attention from theorists within the mesoscopic physics community, where the time-dependent Anderson model is used to describe transport through quantum dots.[18–25]

Recently, we developed a general method[26,27] for the approximate solution to the time-dependent Anderson model using slave bosons. The latter reference[27] (hereafter denoted I) provides a convenient solution of the real-time Dyson equations for the Green's function for the atomic levels. From the real-time Green's functions, both the instantaneous populations as well as the instantaneous spectral distributions can be obtained. These distributions show broad peaks at a position corresponding to the atomic level, and, where appropriate, a Kondo or mixed valence peak near the Fermi level.

In this paper, we investigate how intra-atomic correlation effects influence the velocity dependence of charge-transfer processes in atom-surface scattering by way of the formation of the Kondo or mixed valence peak. Such velocity dependence provides an indirect measure of the time scales for the equilibration of various parts of the electron distributions. We show that the gross structure of the velocity curves is related to the time scale for the formation or decay of the spectral peak at the atomic level position and can be understood from a simple theory neglecting intra-atomic correlation effects. Finer but clearly distinguishable effects arise due to the presence of the much longer time scales associated with the mixed-valence or Kondo peaks. Our calculation thus shows an effect of the nonadiabaticity induced by these many-body features on a quantity that can be measured very directly in an experiment.

II. THE MODEL

The dynamical interaction between an atom and a surface is described by the time-dependent Anderson model,[7,9] as in I:

$$H(t)=\sum_{\kappa}\epsilon_{\kappa}n_{\kappa}+\sum_{a=1}^{N}\epsilon(t)n_a+\frac{1}{2}\sum_{a\neq a'}U_{a,a'}(t)n_an_{a'}+\sum_{\kappa,a}[V_{\kappa,a}(t)c_a^{\dagger}c_{\kappa}+V_{\kappa,a}^{*}(t)c_{\kappa}^{\dagger}c_a]. \quad (1)$$

Here, κ represents the quantum numbers of the states in the substrate band (called $k\sigma$ in I) and a represents the quantum numbers of the atomic states (called $l\sigma$ in I). The appropriately subscripted $c^\dagger$, c, and n are creation, destruction, and number operators for these states. As for the time-dependent quantities, ϵ is the instantaneous energy of the N-fold degenerate atomic level a, U is intra-atomic Coulomb interaction, and $V_{\kappa,a}$ is the tunneling matrix element between a band and an atomic state. Finally, ϵ_κ is the energy of the substrate band state κ.

In the present paper, we will investigate the effects of intra-atomic Coulomb repulsion on the interaction between a single N-fold degenerate atomic level and a metal surface. By this we mean the effects produced by turning on U in Eq. (1). In this model, $N = 1$ corresponds to $U = 0$, i.e., the neglect of intra-atomic correlation effects. For $U = 0$, the Hamiltonian Eq. (1) can be solved analytically in the wide-band limit.[8]

As before, when $N > 1$, we assume that the intra-atomic Coulomb interaction U is sufficiently strong that an N-fold degenerate atomic level with energy $\epsilon(t)$ may only be singly occupied. As previously we use the auxiliary boson technique[28] to enforce this restriction and solve the problem in the fully self-consistent time-dependent noncrossing approximation,[26,27] which is believed to produce an accurate $1/N$ expansion solution for temperatures above an unphysical crossover somewhat lower than the Kondo temperature.[29,30] In the solutions given here, we assume that each of the N degenerate atomic states labeled by a in this paper corresponds to a conserved quantity (e.g., spin).

The instantaneous average populations of the atomic levels is obtained from the equal time argument of a nonequilibrium correlation function $\langle n_a(t)\rangle = G_a^<(t,t)$. The correlation function $G_a^<(t,t')$ is calculated numerically by solving a set of coupled Dyson's equations[27] as in I. The essential input parameters in these equations are the adiabatic positions and widths of the atomic levels, which we model as discussed below, and the substrate band width and temperature.

As an atom approaches a metal surface, the energy levels shift and broaden, thus becoming a function of the time t. The qualitative features of these shifts can be understood from the image interaction between an atom and a perfectly conducting metal surface. This interaction results in the positive ion state shifting upward in the units of eV,

$$\epsilon_P(t) = \epsilon_P^0 + \frac{27.2}{4[Z(t)-1]}, \tag{2}$$

and negative ion state shifting downward in the units of eV,

$$\epsilon_N(t) = \epsilon_N^0 - \frac{27.2}{4[Z(t)-1]}, \tag{3}$$

with decreasing atom surface separation Z, measured in Bohr. The parametrizations in Eqs. (2) and (3) are appropriate for atoms interacting with surfaces that can be modeled using the jellium model.[31] The origin of Z is the jellium edge and the surface charges induced by the atom and electron are assumed to be centered around an image plane at $Z \approx 1$ a.u. To be more specific, the ϵ_P of Eq. (2) is the energy required to add an electron to a positive ion or the negative of the energy to remove an electron from a neutral; on the other hand, the ϵ_N of Eq. (3) is the negative of the energy to remove an electron from a negative ion, or the energy to add an electron to a neutral. In the above expressions (2) and (3), ϵ_P^0 or ϵ_N^0 is the energy of the corresponding atomic level in vacuum. The calculations here take $\epsilon_P^0 - \epsilon_F = -1$ eV and $\epsilon_N^0 - \epsilon_F = +1$ eV, where ϵ_F is the Fermi energy. Stated in words, the positive ion states start below the Fermi and move above it as the surface is approached, while the negative ion states start above the Fermi level and move below it as the surface is approached. Note that Eqs. (2) and (3) as thus parametrized, would be expected to apply to the positive and negative ion states of *different* atomic species.

The full width Γ_a of atomic levels outside metal surfaces typically varies exponentially with atom-surface separation.[31] As discussed in I, the input which determines the tunneling rates and self-energies involves a band average of the tunneling matrix element V and the substrate density of states ρ in the combination $V^2\rho$. We take $V^2\rho$ to be parabolic with half width $D = 5$ eV, with the Fermi level at the center. This means that at the Fermi level Γ_a differs from the band averaged $\bar{\Gamma}_a$ by a factor of 3/2. The precise relationship of the $\bar{\Gamma}_a$ above to the actual adiabatic atomic level width is discussed in detail in I. Our parametrization for $\bar{\Gamma}_a$ is

$$\bar{\Gamma}_a(t) = \bar{\Gamma}^0 \exp\left(-\alpha Z(t)\right), \tag{4}$$

where $\bar{\Gamma}_a$ refers to a single one of the degenerate states labeled by a (labeled by $l\sigma$ in I). We assume that a refers to a conserved quantity such as spin. Here we use the notation

$$\bar{\Gamma} = \sum_a \bar{\Gamma}_a = N\bar{\Gamma}_a. \tag{5}$$

When we vary N we will hold $\bar{\Gamma}$ (*not* $\bar{\Gamma}_a$) constant. The calculations here take $\alpha = 0.65$ Bohr^{-1} and $\bar{\Gamma}^0 = 27.2$ eV, independently as to whether we are considering positive ion or negative ion states, so that we will never need an additional subscript P or N here, as we did when discussing the level shifts. The proposed parametrization is realistic and appropriate for the interaction of the ionization levels and affinity levels of alkali atoms with free-electron metals such as Al or Cu.[31,32]

For atom-surface scattering in the hyperthermal regime it is legitimate to make the classical trajectory approximation. For simplicity, we will assume that the atoms move with constant velocity v, except that the direction of motion is reversed instantaneously during the collision with the surface. This turning point is taken to occur at $Z = 3$ Bohr. Finally in all these calculations, we take the temperature $T = 300$ K.

We will begin the trajectory at $t = -\infty$ with the system in its equilibrium charge state, and calculate the instantaneous population $n(t)$ along the trajectory between $t = -\infty$ and $t = \infty$ as a function of v. In order

to emphasize the nonadiabatic effects that can occur in ion-surface neutralization, we will introduce a quantity $\delta n(t)$, which is related to the instantaneous populations of the atomic levels in the following manner:

$$\delta n_N(t) = n_N(t),$$
$$\delta n_P(t) = 1 - n_P(t). \quad (6)$$

At large distances from the surface, the width of the atomic level is much smaller than the distance between the atomic energy and the Fermi level. The positive ion level is below the Fermi energy and the negative ion state lies above the Fermi energy. For large atom-surface separations and in equilibrium, the positive ion system will therefore be fully occupied (i.e., singly occupied) and the negative ion system will be totally empty. The corresponding values of δn are therefore zero. Since the initial conditions are chosen such that $\delta n(-\infty)=0$, $\delta n(\infty)$ is a measure of the nonadiabaticity in the charge-transfer process.

For $v \to 0$, the system remains in equilibrium throughout the trajectory and $\delta n(\infty) \to 0$, in other words the system is adiabatic. For finite v, $\delta n(\infty)$ is not zero, and hence the system is nonadiabatic. In simple models often used to treat charge transfer (e.g., $U = 0$), the time scale relevant for the onset of nonadiabatic behavior is determined by the inverse of the level width Γ_a. We will show here that a longer time scale generated by intra-atomic correlation effects can also significantly affect this nonadiabatic charge transfer at low v.

III. RESULTS AND DISCUSSION

The input parameters used in the calculation of this paper for the positive and negative ion states provide examples of what we denote as *conjugate* atom-surface systems. We will refer to a pair of negative and positive ion states as *conjugate* to each other if the following conditions are satisfied: (i) the conduction band in the substrate is symmetric with respect to the Fermi energy, (ii) the adiabatic atomic level widths as a function of Z are the same, (iii) the level shifts of the atomic states are mirror images of each other with respect to the Fermi energy. By comparing the results for conjugate systems with and without Coulomb interaction, it is possible to directly assess the role of many-body effects on nonadiabatic charge transfer.

The reason for this is the particle-hole symmetry in the simple model being considered. To discuss this, we must make clear how we are going to apply Eqs. (2) and (3). Let us assume the degeneracy index a refers to the z component of spin. Then (2) is taken to refer to the energy to add an electron to a positive ion, whose state in the absence of the electron would be spinless. The effect of large intra-atomic Coulomb interaction is to prevent the presence of still another electron, in other words to prevent a negative ion state. On the other hand, (3) is taken to refer to the energy to add an electron to a neutral atom (of a different species), whose state in the absence of the electron would be spinless. Here, the effect of large intra-atomic Coulomb interaction is to prevent the presence of still another electron, in other words, to prevent a doubly charged negative ion state. Thus, the presence of this type of intra-atomic Coulomb interaction breaks the particle-hole symmetry implicit in points (i)–(iii) of the above paragraph. [Note, however, that the particle-hole symmetry would not be broken if the negative ion state in (3) were a spin zero state of N interacting electrons; in that case the effect of large intra-atomic Coulomb interaction would be to prevent more than one *hole* from occurring, an effect that is the exact conjugate of the assumption we make for the positive ion state in (2).]

In our case then, particle-hole symmetry occurs only for $N = 1$, where intra-atomic Coulomb interaction U has no effect. In that case if the initial condition that the positive and negative ion states are populated satisfies $n_N(t = -\infty) = 1 - n_P(t = -\infty)$ the theory predicts that the instantaneous populations $\delta n_N(t) = \delta n_P(t)$. However, for our choice of states, this symmetry is broken by the intra-atomic Coulomb interaction for $N > 1$. The difference between $\delta n_N(t)$ and $\delta n_P(t)$ thus provides a direct estimate of the influence of many-body effects. [Note that for the $N = 1$ case, we use the noninteracting theory ($U = 0$), rather than the $N = 1$ version of the auxiliary boson theory, because the latter still has small spurious remnants of the many-body effects.]

In order to understand the effects of intra-atomic repulsion on the interaction between an atom and a metal surface it is useful to study the equilibrium spectral function of the atomic state.[27] In Fig. 1, this spectral function is plotted for four different atom surface separations for the negative ion state interacting with the surface for large intra-atomic Coulomb interaction and for a sys-

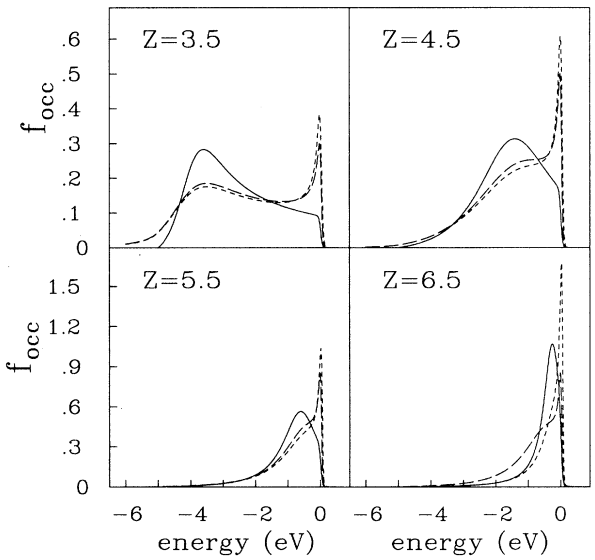

FIG. 1. Spectral function for a negative ion state interacting with a surface for some different atom-surface separations. The parametrization of the atomic levels is as Eqs. (3) and (4). The solid lines are the $U = 0$ results. The dashed lines are the results for $N = 2$ and the dotted lines are the results for $N = 4$.

tem with $U = 0$. The figure illustrates the fundamental influence of intra-atomic correlation on the interaction between an atom and a metal surface. For small atom-surface separation, the spectral functions for large intra-atomic interaction exhibit two distinct peaks, the atomic level resonance and the Kondo resonance near the Fermi energy. For the case where $U = 0$, only the atomic level peak is present. The atomic level peak represents the hybridized atomic state and its width is equal to Γ. The Kondo peak is a many-electron effect and is due to the interaction of degrees of freedom provided by the N-fold degeneracy and the substrate electrons. At low temperature the Kondo peak occurs at an energy $\approx T_L$ above the Fermi level and has a width $\approx 2\pi T_L/N$, where T_L sets the low energy scale and is roughly equal to the Kondo temperature T_K (see Appendix). For temperatures above $\sim T_L$ the Kondo peak weakens and disappears. For larger atom surface separation, the negative ion state shifts above the Fermi energy. When this happens, the Kondo peak disappears, and only a tail of the atomic level peak extends below the Fermi energy.

In Fig. 2, the spectral function for a positive ion state interacting with a surface is shown for the same atom-surface separations as shown in Fig. 1. It can clearly be seen that the spectral functions look very different from those in Fig. 1. For small atom-surface separations, the atomic level lies above the Fermi energy and the spectral function is relatively featureless. For larger atom-surface separations, the atomic level has shifted below the Fermi energy and many-body effects become important. Since the width Γ is relatively small at large atom-surface separations, T_K is small and the Kondo peak is very narrow.

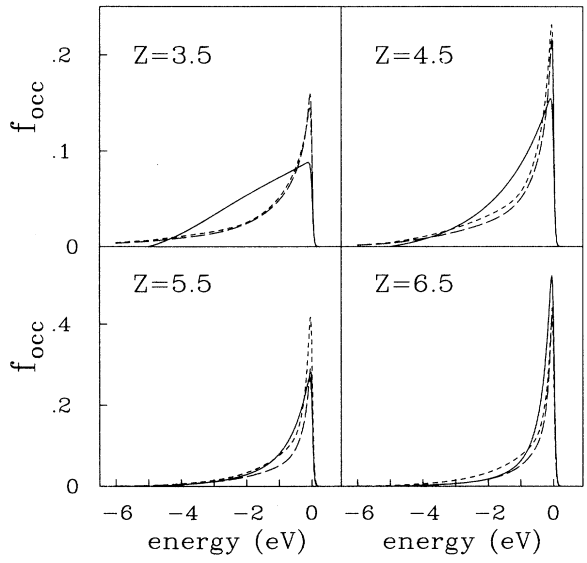

FIG. 2. Spectral function for a positive ion state interacting with a surface for some different atom-surface separations. The parametrization of the atomic levels is as Eqs. (2) and (4). The solid lines are the $U = 0$ results. The dashed lines are the results for $N = 2$ and the dotted lines are the results for $N = 4$.

The principal purpose of the present paper is to illustrate a source of nonadiabaticity in charge transfer introduced by a particular many-electron effect, that is the formation of the Kondo or mixed-valence state. Before doing this, we will discuss some of the most trivial aspects of nonadiabaticity that are present in any charge-transfer reaction in an atom-surface scattering event.

These simple aspects are most easily illustrated by the simple master equation appropriate for charge transfer,[26] which provides a convenient method for the qualitative estimate of charge-transfer probabilities in a atom-surface scattering in the hyperthermal regime:

$$\frac{dn(t)}{dt} = -\frac{\Gamma(t)}{N}[1 - f(\epsilon(t))]n(t) + \Gamma(t)f(\epsilon(t))[1 - n(t)], \tag{7}$$

where $n(t) = \sum_a \langle n_a(t)\rangle = N\langle n_a(t)\rangle$ is the sum of the mean populations of the N-fold degenerate atomic level, and $\epsilon(t)$ is given by either (2) or (3) as appropriate, and where $f(\epsilon)$ is the Fermi function at temperature T. The quantity $\Gamma(t)$ is the golden rule tunneling rate, which for our assumed parabolic shape for $V^2\rho$ is given by

$$\Gamma(t) = \frac{3}{2}\left[1 - \left(\frac{\epsilon(t) - \epsilon_F}{D}\right)^2\right]\bar{\Gamma}(t), \tag{8}$$

where $\bar{\Gamma}(t)$ is defined by Eqs. (4) and (5). The second term in the brackets in (8) plays a negligible role in the considerations below. For $T = 0$ K, and for velocities $v < 0.1$ a.u., the approximate solutions to this equation for positive and negative ions are

$$\delta n_P(\infty) = \exp\left(-\frac{\Gamma(t_c)}{\alpha v}\right),$$
$$\delta n_N(\infty) = \exp\left(-\frac{\Gamma(t_c)}{N\alpha v}\right), \tag{9}$$

where $\Gamma(t_c)$ is the width of the atomic level when it crosses the Fermi level. These solutions follow, because at these velocities memory of what happened on the ingoing trajectory is essentially lost: the final population $n_P(\infty)$ is dominated by the refilling of the atomic levels at a rate Γ right after the downward Fermi level crossing, while $n_N(\infty)$ is dominated by a reemptying of the levels at a rate $\Gamma_a = \Gamma/N$ right after the upward Fermi level crossing. In Fig. 3, the final charge transfer representing the exact solution of (7) for $\delta n(\infty)$ is plotted as a function of inverse velocity for $N = 1$, 2, and 4. Since the $N = 1$ ($U = 0$) Hamiltonian preserves electron-hole symmetry, the results for the two conjugate systems are identical. From the figure, it can clearly be seen that intra-atomic Coulomb interaction breaks the electron-hole symmetry. The larger N is, the larger difference is seen between δn_P and δn_N. The figures shows that the variation of $\delta n_P(\infty)$ with inverse velocity is an approximately exponential function as would be expected from Eq. (9).

A characteristic feature of the solutions to Eq. (7) as shown in Fig. 3, is the almost perfect exponential dependence of $\delta n(\infty)$ on $1/v$. This dependence is caused

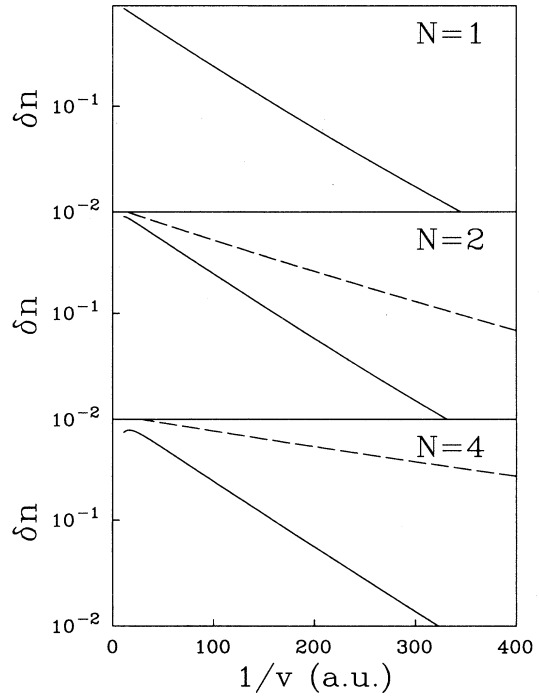

FIG. 3. Calculated δn_p (solid line) and δn_N (dashed line) as a function of velocity for $N = 1$, $N = 2$, and $N = 4$, using the master equation, Eq. (7). The substrate temperature is $T = 300$ K.

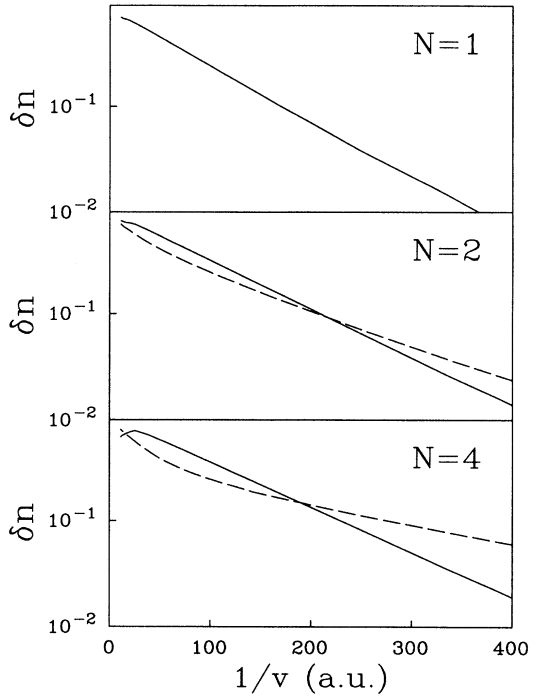

FIG. 4. Calculated δn_p (solid line) and δn_N (dashed line) as a function of velocity for $N = 1$, $N = 2$, and $N = 4$, using the exact solution of the coupled Dyson equations (see I). The substrate temperature is $T = 300$ K.

by the fact that only a single time scale influences the charge transfer. This feature persists in the exact solution discussed below for those cases where the Kondo peak cannot form, and hence where there is but a single time scale determined by the inverse width of the atomic state for $t \approx t_c$. Thus, the master equation provides a simple intuitive and analytic way to understand this exponential dependence.

We now turn to the numerical solution of Eq. (1). In Fig. 4, we show the same curves calculated using the full coupled Dyson's equations of paper I, without making the master equation approximation. The $N = 1$ curves correspond to $U = 0$, i.e., the neglect of intra-atomic correlation effects. As expected for this case $\delta n_N(\infty) = \delta n_P(\infty)$ for all velocities. The calculated δn for $N = 1$ represents an exact solution of the charge-transfer problem neglecting intra-atomic correlation. It can clearly be seen that the charge transfer can be described by a single exponential function of inverse velocity and is very similar to the curves presented in the upper panel of Fig. 3.

The two lower panels in Fig. 4 show the calculated $\delta n_P(\infty)$ and $\delta n_P(\infty)$ in the presence of intra-atomic interaction. Again the final positive ion populations vs $1/v$ follow qualitatively the straight lines on a log plot shown by the master equation calculation, indicating the importance of but a single rate, related to the width of the atomic level peak. The plot of the negative ion population, on the other hand, exhibits a clear nonlinear behavior. For low velocities, the decrease of n_N with velocity is considerably smaller than at the large velocities. This result is very different from the rate equation result Eq. (7) and cannot be understood from the master equations, but only by understanding the influence of the additional rates involved in the formation of the Kondo peak.

In order to provide further understanding of this feature, the instantaneous population on the negative ion state is plotted along the trajectories for different velocities in Fig. 5. The equilibrium population is symmetric around the turning point as expected. The levels cross the Fermi energy at a distance $Z = 7.8$ a.u. The increase in the population near the turning point is due to the downshift of the atomic level. It can be seen that the instantaneous populations $n_N(Z)$ follows the equilibrium population relatively closely. For the large velocity the population and depopulation of the atomic levels is shifted slightly to the right due to the reduction in the effective tunneling rates at large velocities. The equilibrium population for the $N = 4$ case looks relatively similar to the $N = 1$ case. Although the spectral functions look very different, the integrated population of the atomic level is relatively independent of N when the level lies below the Fermi energy. The instantaneous populations for the $N = 4$ situation looks very different. A clear asymmetry is induced even at the lowest velocities. The total final population for the $U = 0$ case ($N = 1$) is larger than for the large U case ($N = 4$) at high velocity ($v = 0.02$ a.u.), but smaller for low velocity ($v = 0.003$ a.u.). The reason for this asymmetry and velocity dependence of the final population can be understood from the

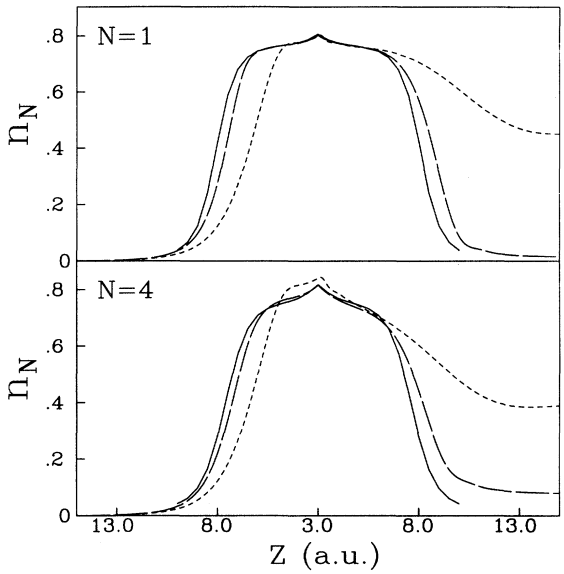

FIG. 5. Instantaneous population of the negative ion state along the trajectory for different degeneracy and velocities. The upper part of the figure refers to $N = 1$ and the lower part is $N = 4$. The solid line is the results for equilibrium. The dashed lines are for $v = 0.003$ a.u. and the dotted line is for $v = 0.02$ a.u.

spectral function of the atomic states.

An effect of intra-atomic correlation is to reduce the weight of the broad atomic level peak and introduce spectral weight in the Kondo peak. The time scale for formation and decay of the atomic level peak and the Kondo peak is very different.[27,33] At the largest velocities, the Kondo feature cannot be formed. The population of the negative ion state contributed by the broad atomic level peak is smaller for the large U case ($N = 4$) than for the $U = 0$ case ($N = 1$). This difference persists when the atom leaves the surface. The dynamics of the negative ion state is, therefore, characterized by the fast atomic level time scale. For low velocities, the Kondo feature is formed during the outgoing trajectory. This enhances the negative ion population near the surface. Because of the slower rate of depopulation for the Kondo peak, the final population of the negative ion state is largely formed from the weight of this peak. Therefore, the final population for the large U case ($N = 4$) is larger than that for the $U = 0$ case ($N = 1$). This enhancement due to the formation of the Kondo peak causes the break in the plots of δn_N, as a function of inverse velocity for the lowest velocities. The multiple slopes shown in logarithm of δn as a function of inverse velocity for negative ion states provide a signature for the Kondo peak due to intra-atomic correlation.

ACKNOWLEDGMENTS

This work is supported in part by the National Science Foundation under Grant Nos. DMR 91-17479 (PN,HS) and DMR 94-07055 (DCL). Acknowledgment is made to the donors of the Petroleum Research Fund, administered by the American Chemical Society for the partial support of this research, under Grant No. 27240-AC5 (PN,HS).

APPENDIX A: THE LOW ENERGY SCALE

Here, we summarize some known results about the low energy scale relevant to the discussion in this work. Excellent reviews[29,30] exist.

The energy (or temperature) T_L characterizing this scale is related to the Kondo temperature through $T_L = T_K/w_N$, where $w_N = e^{(1+C-3/2N)}/2\pi\Gamma(1+1/N)$ is the N dependent Wilson number, which is of order unity. Here, Γ is the gamma function and $C = 0.577\ldots$ is Euler's constant. For a square band ($V^2\rho$) of width $2D$, T_K can be obtained analytically[29] by Bethe ansatz with the result

$$T_K = \frac{D}{2\pi}\exp\left(1+C-\frac{3}{2N}\right)\left(\frac{N\Gamma_a}{2\pi D}\right)^{1/N} \times \exp\left(-2\pi\frac{|\epsilon-\epsilon_F|}{N\Gamma_a}\right), \quad \text{(A1)}$$

where here $\Gamma_a = \frac{3}{2}\bar{\Gamma}_a$; see Eq. (5) and the discussion leading to it. For the parabolic band used in the calculations in this paper, the D to be used in (A1) should be reduced; an estimate for this reduction is given in I. The expression for T_K given in I was appropriate to the case where $|\epsilon - \epsilon_F| > eD$. Equation (A1) on the other hand is appropriate for the case where the above inequality is reversed. Both expressions assume that one is in the Kondo region characterized by $\langle n_a\rangle \sim 1$.

[1] G. A. Kimmel, D. M. Goodstein, Z. H. Levine, and B. H. Cooper, Phys. Rev. B **43**, 9403 (1991).
[2] M. S. Hammond, F. B. Dunning, G. K. Walters, and G. A. Prinz, Phys. Rev. B **45**, 3674 (1992).
[3] P. D. Johnson, A. J. Viescas, P. Nordlander, and J. C. Tully, Phys. Rev. Lett. **64**, 942 (1990).
[4] A. L. Johnson, S. A. Joyce, and T. E. Madey, Phys. Rev. Lett. **61**, 2578 (1988).
[5] C. C. Hsu, H. Bu, A. Bousetta, J. W. Rabalais, and P. Nordlander, Phys. Rev. Lett. **69**, 188 (1992).
[6] J. Los and J. J. C. Geerlings, Phys. Rep. **190**, 133 (1990).
[7] P. W. Anderson, Phys. Rev. **124**, 41 (1961).
[8] A. Blandin, A. Nourtier, and D. Hone, J. Phys. (Paris) **37**, 369 (1976).
[9] R. Brako and D. M. Newns, Rep. Prog. Phys. **52**, 655 (1989).
[10] W. Bloss and D. Hone, Surf. Sci. **72**, 277 (1978).
[11] T. B. Grimley, V. C. J. Bhasu, and K. L. Sebastian, Surf.

Sci. **124**, 305 (1983).
[12] A. Yoshimori, H. Kawai, and K. Makoshi, Prog. Theor. Phys. Suppl. **80**, 203 (1984).
[13] K. L. Sebastian, Phys. Rev. B **31**, 6976 (1985).
[14] R. Brako and D. M. Newns, Solid State Commun. **55**, 633 (1985).
[15] H. Kasai and A. Okiji, Surf. Sci. **183**, 147 (1987).
[16] K. W. Sulston, A. T. Amos, and S. G. Davison, Phys. Rev. B **37**, 9121 (1988).
[17] J. B. Marston, D. R. Andersson, E. R. Behringer, and B. H. Cooper, Phys. Rev. B **48**, 7809 (1993).
[18] C. Liu and Q. Niu, Phys. Rev. B **47**, 13 031 (1993).
[19] G. W. Bryant, Phys. Rev. B **48**, 8024 (1993).
[20] C. A. Stafford and S. Dassarma, Phys. Rev. Lett. **72**, 3590 (1994).
[21] A. D. Stone and H. Bruus, Surf. Sci. **305**, 490 (1994).
[22] C. Bruder and H. Schoeller, Phys. Rev. Lett. **72**, 1076 (1994).
[23] P. A. Maksym and T. Chakraborty, Phys. Rev. Lett. **65**, 108 (1992).
[24] N. S. Wingreen and Y. Meir, Phys. Rev. B **49**, 11 040 (1994).
[25] A.-P. Jauho, N. S. Wingreen, and Y. Meir, Phys. Rev. B **50**, 5528 (1994).
[26] D. C. Langreth and P. Nordlander, Phys. Rev. B **43**, 2541 (1991).
[27] H. Shao, D. C. Langreth, and P. Nordlander, Phys. Rev. B **49**, 13 929 (1994), abbreviated I.
[28] P. Coleman, Phys. Rev. B **29**, 3035 (1984).
[29] A. C. Hewson, *The Kondo Problem to Heavy Fermions* (Cambridge University Press, Cambridge, 1993).
[30] N. E. Bickers, Rev. Mod. Phys. **59**, 845 (1987).
[31] P. Nordlander and J. C. Tully, Phys. Rev. B **42**, 5564 (1990).
[32] P. Nordlander, Phys. Rev. B **46**, 2584 (1992).
[33] H. Shao, P. Nordlander, and D. C. Langreth (unpublished).